Double opponency as a generalized concept in texture segregation illustrated with stimuli defined by color, luminance, and orientation

Andrei Gorea

Laboratoire de Psychologie Expérimentale, René Descartes University and Centre National de la Recherche Scientifique, 28 rue Serpente, 75006 Paris, France

Thomas V. Papathomas

Laboratory of Vision Research and Department of Biomedical Engineering, Rutgers University, New Brunswick, New Jersey 08903

Received July 9, 1992; revised manuscript received December 29, 1992; accepted January 4, 1993

We present a series of experiments in texture discrimination with textures whose local elements are defined by their color (red and/or green), luminance polarity, and orientation (vertical and/or horizontal). The 23 distinct texture configurations were designed for testing and parameterizing a model based on the generalization of the concept of double opponency. The double-opponent mechanisms of the model are classified into four domains: the luminance- and color-oriented (LO and CO) domains and the luminance- and color-nonoriented (LnO and CnO) domains. Texture edge strength is extracted from the weighted, half-wave rectified outputs of each double-opponent mechanism. These signals are then combined through probability summation within each domain. Overall sensitivity to a given texture pair is predicted by the probability summation of all the domain outputs. Good fits of the experimental data are obtained when the contribution of the CO domain is the smallest and the contribution of the CnO domain is the largest. We suggest that the double-opponency principle is a natural way of implementing spatial interactions in higher-order domains and that it could be generalized to other dimensions such as spatial frequency, motion, and stereopsis.

1. INTRODUCTION

The concept of double opponency may be traced back to Hering[1] and was explicitly used in accounts of the behavior of a class of color-sensitive cells in the goldfish retina[2] and in area V1 of the monkey visual cortex.[3] Jameson and Hurvich were among the first to elaborate on the concept as it is related to psychophysical data; see Jameson.[4] A chromatic double-opponent cell will display a response increment if it is stimulated with red and green lights in the center and in the surround of its receptive field, respectively, and a response decrement if the spatial positions of the two lights are interchanged [see Fig. 1(a)].

With this prototypical idea of double opponency in mind, one may overlook the fact that a linear, spatially opponent achromatic (i.e., Kuffler) unit can be looked on as a double-opponent unit in the luminance-polarity domain [Fig. 1(b)]. If such behavior is achieved by subtraction of the half-wave rectified outputs of independent ON and OFF achromatic subunits (e.g., Ref. 5 and Fig. 7 therein), the relationship between chromatic and luminance double opponencies is more than just analogical. Of course, there is no *a priori* reason not to extend the double-opponency principle to second-order dimensions such as orientation (and spatial frequency). A first-order oriented unit, for example, is double opponent insofar as luminance polarity is concerned, but it is not double opponent in the orientation domain *per se*. A double-opponent oriented (second-order) unit would have a receptive field center that receives opposite-sign inputs from first-order oriented units with overlapping receptive fields tuned to different (e.g., 45° apart) orientations. The surround of such a second-order unit would receive inputs from first-order oriented units with their signs reversed relative to the center. This idea is illustrated in Fig. 1(c).

The essential property of a double-opponent unit is to measure generalized spatial contrast. The notion of generalized contrast refers here to the fact that contrast can be measured in any dimension, from luminance to orientation or spatial frequency, etc. The critical characteristic of such an operator is its spatially opponent behavior rather than its linearity: the information provided by two half-wave rectified double-opponent units of opposite polarities is equivalent to the information provided by a fully linear, spatially opponent unit (e.g., Ref. 5). Given that half-wave rectification characterizes most of the striate cells, double-opponent units in the classical sense might be difficult to find.[6]

The main message conveyed by Fig. 1 is that all the standard models of texture discrimination do in fact use first-order (luminance) double-opponent kernels as a first processing stage.[7–13] None of them, however, extended the double-opponency concept (in the sense defined above) to second-order dimensions such as orientation[14] and spatial frequency. However, the existence of spatial interactions among first-order (oriented, spatial frequency) filters has been known for some time,[15] and these interactions have recently received both psychophysical[16–18] and physiological[19–21] support. Moreover, these models addressed only discrimination issues in the luminance domain, and little

0740-3232/93/071450-13$06.00

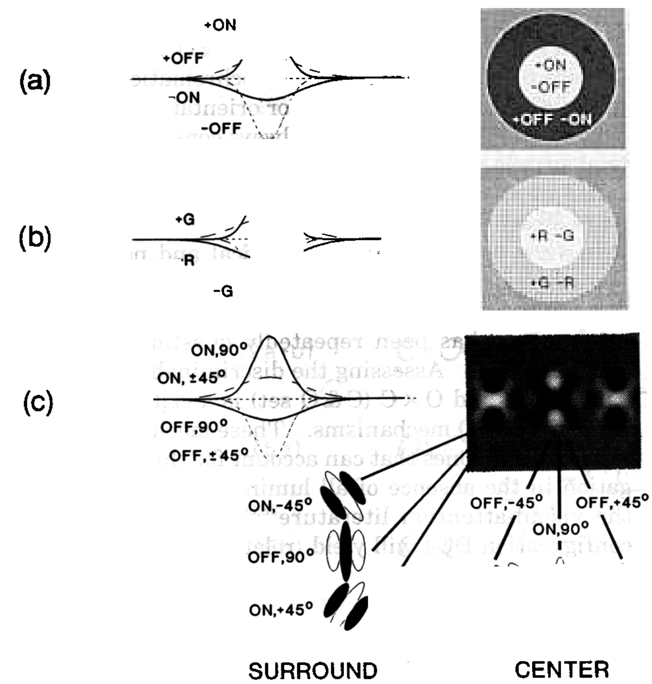

Fig. 1. Generalized double opponency. (a) Classical, ON-center, OFF-surround receptive field (RF) that is both nonoriented and achromatic. If one assumes independent ON and OFF systems, such a unit can be looked on as double opponent in the polarity domain. This interpretation is made explicit on the left-hand side, where the response profile of this RF is shown. (b) Typical chromatic, double-opponent RF. A unit of this type responds positively to a red (R) light in its center and to a green (G) light in its surround and reverses polarity when the positions of the two lights are reversed. (c) Hypothetical double-opponent RF in the orientation domain that responds to either luminance or chromatic contrasts. In its center such a unit will respond positively to a vertical bar of a given polarity (e.g., bright or R) and negatively to a ±45° bar of the same polarity. Responses are reversed in its surround. Note that the linear superposition of the two groups of three RF's (in the center and the surround) results in many ON and OFF lobes of different strengths that are reminiscent of the RF of a complex cell.

is known of how they would behave if they were applied to chromatically defined textures or to both chromatically defined and luminance-defined textures.[22,23]

The purpose of the present study was to test the predictions of a generalized double-opponent model against texture discrimination performances measured with a large variety of texture pairs built from texture elements—or textels—defined by their luminance and/or chromatic contrast and their orientation. A first set of stimuli involved only color (red and green) and orientation (vertical and horizontal) attributes. A second stimulus set involved luminance-polarity and orientation attributes and was designed as a template against which one could evaluate the efficiency of the chromatic channels in texture discrimination. Finally, a third group was constructed by the combination of luminance-polarity and chromatic attributes. One of the particular interests here was to evaluate, by means of the proposed model, the relative contributions of the four mechanism groups that were described in previous studies[22,24] [i.e., color-oriented (CO), color-nonoriented (CnO), luminance-oriented (LO), and luminance-nonoriented (LnO)] and that were presumably involved in tasks of this kind.

The main novelty of the model presented here consists in the use of double-opponent interactions across color and orientation. With only five free parameters, this generalized double-opponent model provides a fairly good fit to the psychophysical data, which suggests that some pop-out effects traditionally studied in the visual-attention literature (see Ref. 25 for a review) could be accounted for at a relatively early stage of visual processing. The good fit of the data encourages us to think that the concept of double opponency might be successfully applied to domains other than orientation, such as spatial frequency, stereopsis, and motion (for the last-named domain see Refs. 26 and 27).

2. METHODS

A. Stimuli

Stimulus Configurations and Notation

We present data obtained with two sets of stimulus configuration. The first set, shown schematically in Fig. 2, consisted of equiluminant texture pairs that could be discriminated exclusively on the basis of color and/or orientation differences (the C & O set). The red and/or green textels were displayed on an equiluminant background. Given the following three construction constraints, the C & O set represents a quasi-exhaustive sample of all possible stimulus configurations:

(1) Textures were exclusively composed of red (filled symbols) and/or green (open symbols) rectangular textels displayed either vertically or horizontally. Only the configuration at bottom right in Fig. 2 was composed of square textels.

(2) Texture density was kept constant across all the textures.

(3) Each texture in a texture pair was built of at most four distinct textel types. When more than one textel type was employed, textel types were always equally represented (i.e., the population density of each was $1/n$, where n was the number of different types).

There are 11 texture pairs in Fig. 2, of which five have been labeled with a trigraphic notation by analogy with our notation in previous motion and texture grouping studies.[22,24] This notation will serve as a mnemonic and will facilitate description and comparison of the data. The first letter of the trigraphic notation denotes the attribute on which discrimination is based, i.e., C or O for the C & O set. The second letter specifies whether the second attribute, denoted by the third letter of the trigraph, is uniform across the two textures to be discriminated [within (w)], varies randomly [across (×)], or covaries positively with the first attribute [plus (+)]. For example, the notation O w C (orientation within color) indicates that the texture pair is discriminated on the basis of an orientation difference, while the color is constant within the whole texture. C × O denotes that discrimination is based on a color difference, while orientation varies randomly across the whole texture. Finally, C + O signifies that discrimination is jointly based on a color and an orientation difference. The labels SCJ for configuration 4 and DCJ for configuration 6 stand for simple conjunction and double conjunction, respectively, since these configu-

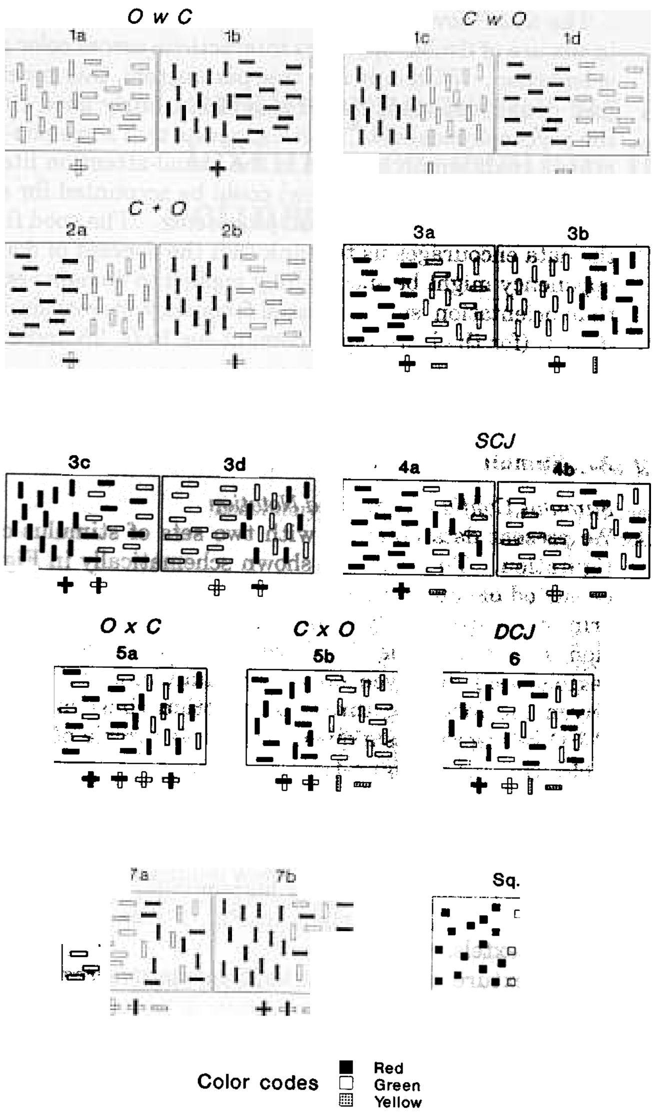

Fig. 2. Schematic illustration of the texture pairs used in the complete C & O set. Below each texture pair are shown the textels that compose the specific masks (M1 type) with which they are associated. Each texture pair is labeled with an alphanumeric code used throughout. Texture pairs 1a and 1b, 1c and 1d, 2a and 2b, 4a and 4b, 5a, 5b, and 6 are also labeled with a trigraphic code explained in the text. Color codes are given at the bottom of the figure. Textels were always presented on a yellow background, with which they were equiluminant. Yellow textels were present only in the mask, and their luminance was twice that of the yellow background.

rations are constructed on the same basis as the classical SCJ and DCJ stimuli of Treisman and Gelade.[28]

There are several configuration pairs for which there is no *a priori* reason for expecting different performances. For example, texture segregation in both cases 1a and 1b is due to orientation differences of green (case 1a) and red (case 1b) textels (O w C). Similarly, in cases 2a and 2b segregation is attributed to both color and orientation differences (C + O). The other cases for which performances are expected to be the same are 3a and 3b, 3c and 3d, 4a and 4b, and 7a and 7b. Since this expectation was verified by the experimental data, performances were averaged across the corresponding condition pairs.

All configurations labeled with the trigraphic notation in the C & O set (including DCJ) were reproduced for combinations of polarity and orientation (P & O) and color and polarity (C & P) attributes. The P & O set consisted of texture pairs constructed with isochromatic (yellow) textels of different polarities and/or orientations. The C & P set consisted of texture pairs always constructed with vertical textels of different colors and/or polarities. A new series of experiments was then run with the 18 texture pairs shown in Fig. 3.

In view of both neurophysiological and psychophysical studies, some of the texture pairs illustrated in Figs. 2 and 3 have an *a priori* significance. The existence of CO mechanisms has been repeatedly questioned by neurophysiologists.[29] Assessing the discriminability of texture pairs O w C and O × C (C & O set) is a critical test of the existence of CO mechanisms. These mechanisms are, indeed, the only ones that can account for this type of segregation in the absence of all luminance cues. In view of the visual-attention literature[28,30,31] it is expected that configuration DCJ will yield relatively weak segregation performances.

Stimulus Characteristics

The texture pairs shown in Figs. 2 and 3 were displayed on a Mitsubishi HL69155ATK monitor screen driven by a Silicon Graphics IRIS workstation. Each texture pair had its corresponding noise texture (referred to as matched noise), where the textels of both textures in the texture pair were randomly intermixed across the screen, which consequently produced a uniformly textured area.

At 122 cm from the observer the inspection field subtended 16.9° × 13.2°. Textels were 0.07° wide and 0.38° long and covered approximately 7.5% of the inspection field (28 × 23 textels presented simultaneously). They were always displayed on a yellow background of approximately 24 cd/m^2. The Commission Internationale de l'Eclairage x and y coordinates of the red and green textels were (0.65, 0.31) and (0.29, 0.59), respectively. Yellow textels and background were obtained by the linear combination of the red and green hues set at equiluminance by means of flicker photometry (for the details see Ref. 24). The luminance contrast used in producing polarity differences for the P & O and C & P stimuli was chosen in a preliminary experiment so that it matched discrimination performances obtained with configurations C w O and P w O (see Subsection 2.B). The best match was obtained for a luminance contrast of approximately ±10%. A central yellow, bright cross of the size of the textels was used for steady fixation.

Texture pairs were constructed so that they randomly displayed either a vertical (as illustrated in Figs. 2 and 3) or a horizontal edge. In order that all local cues were avoided, the edge itself was wavy and randomly displaced within a ±1° range with respect to the fixation point.

In the first series of experiments (C & O set) a specific mask (hereafter referred to as M1) was designed for each texture pair (see Fig. 2). The design principle was to provide mask elements that represented the pairwise combination of all textel types that composed a given texture pair. For example, the mask for configuration 6 (DCJ) was composed of red and green crosses and vertical and horizontal yellow textels, which represent all possible pairwise combinations of textels taken from the left-hand and right-hand regions of the texture pair. Red and

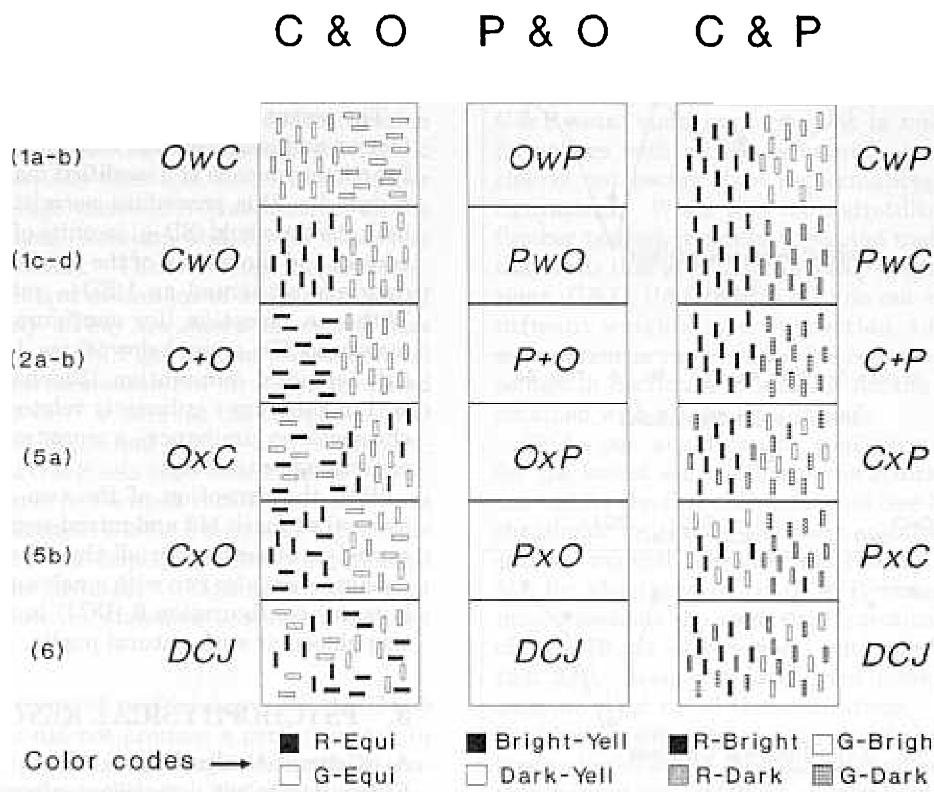

Fig. 3. The eighteen texture pairs used in the second set of experiments are grouped by sixes in forming C & O, P & O, and C & P sets. When we use black and white textels to signify either color (red or green) or polarity, the P & O set is strictly identical to the C & O set and is not shown here. Color codes are shown at the bottom of the figure for each set. Texture pairs are labeled with both alphanumeric and trigraphic notations (from Fig. 2).

green crosses were matched in luminance with the target textels, while the vertical and horizontal yellow bars were approximately twice as bright as the background. M1 was thus stimulus dependent. Since mask element types were selected randomly, the spatial matching between a textel in the texture pair and its corresponding mask element was not necessarily preserved.

The use of mask M1 does not guarantee that all texture pairs in the C & O set are equally masked. To test this possibility, we used two additional mask types. In the second set of experiments (stimuli shown in Fig. 3) the mask configuration was homogeneous over all 18 stimulus configurations (i.e., stimulus independent). The mask (hereafter referred to as M2) consisted of nonoverlapping textels whose color (red or green), polarity (bright or dark), and orientation (vertical or horizontal) were randomly chosen across space and across trials. Thus any particular texture pair was masked by the random combination of all attributes used in the three stimulus sets (i.e., C & O, P & O, and C & P). Observer AG ran selected conditions from the C & O set with a third mask (hereafter referred to as M3) composed exclusively of yellow crosses, i.e., the linear sum of all possible textels used in that particular set. This pure luminance mask (also stimulus independent) had twice the luminance of the individual target textels (i.e., 100% contrast relative to the yellow background). Note that high-contrast, pure luminance stimuli may efficiently mask pure chromatic stimuli.[32]

Mask elements always occupied the same spatial positions as those of the textels of the texture pair and of its matched noise.

B. Procedure

In order to compare performances obtained with pure chromatic (i.e., equiluminant) and pure luminance (i.e., equichromatic) stimuli, one needs to set them at equivalent contrasts. The yellow, bright, and dark textels were set at their equivalent luminance contrast relative to the red–yellow and green–yellow chromatic contrasts by means of the following procedure (for more details see Ref. 33). Percentages of correct detection (see below) for the C w O stimulus were first measured at a fixed stimulus duration as a function of the overall size of the inspection field, which yielded a classical psychometric function. The window size that yielded detection performances of approximately 80% was chosen for use with the P w O configuration, and performances were measured this time as a function of luminance contrast with the same stimulus duration. The luminance contrast that yielded the same percentage correct detection as that in the C w O experiment (i.e., 80%) was named the equivalent luminance contrast and used throughout. Both window-size-dependent and contrast-dependent measurements were performed without masks. Note that this procedure equates the total activities in the CnO and CO mechanisms on the one hand and in the LnO and LO mechanisms on the other hand. It does not guarantee, therefore, that the activities of each subset in the chromatic and luminance domains are pairwise matched.

For subsequent experiments a typical trial proceeded as follows. A texture pair and its matched noise (i.e., the random combination of all textels of the texture pair) were presented each in one of two temporal intervals for the

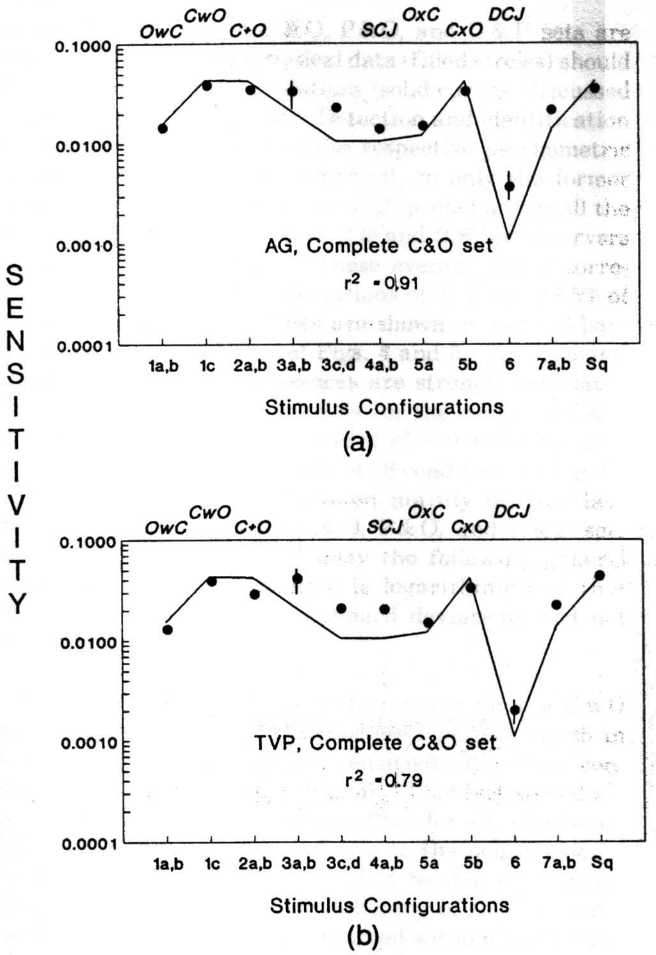

Fig. 4. Sensitivities (filled circles), measured in units of inverse milliseconds, and simulations (solid curves) for the 11 texture pairs in the complete C & O set and for the two observers, (a) AG and (b) TVP. Alphanumeric and trigraphic notations are shown on the abscissas. The inset in each plot gives the correlations between data and simulations. Vertical bars show the average ±1 standard deviation as computed from the average slope of the psychometric functions fitted to the data of each observer.

same duration (SD, for stimulus duration). Within each interval the texture pair and the noise were followed after a fixed interstimulus interval (16.7 ms) by the mask stimulus. The duration of the mask was 333 ms.

The percentage correct as a function of SD was measured by means of a 2 × 2 alternative forced-choice, constant-stimuli procedure in which the observer indicated both the temporal interval that contained the target (detection) and the orientation of the texture edge (identification). Pilot experiments were required for the choice of four or five SD's, which bracketed the threshold for each texture pair. Most of the experiments were run with a fixed stimulus configuration in each session (blocked sessions), which was randomized across sessions. Within a blocked session a given texture pair (and its matched noise and mask) was presented at least 50 times per SD, so that a complete session consisted of at least 200 (or 250) trials. Each stimulus condition was repeated at least twice, so that each percentage correct (for a given SD, configuration, and stimulus set) was computed out of at least 100 trials. In order to ensure that the data collected in the blocked sessions were not biased by nonsensory effects (i.e., stimulus-specific response strategies), observer AG also ran the C & O set with stimulus configurations randomized within sessions (mixed sessions). These data were obtained with the mask M1 only.

The percentages correct as a function of SD for both detection and identification tasks were fitted with a Weibull function by means of a modified maximum-likelihood procedure.[34] This procedure permitted the assessment of both the threshold (SD_{TH}, in units of milliseconds) at 81.6% correct and the slope β of the psychometric function. The data are presented as $1/SD_{TH}$ ratios (i.e., sensitivity). With one exception [for configuration 6 (DCJ)] all the measured SD_{TH} were below 90 ms, i.e., within the range of full temporal summation (Bloch's law).[35] Thus SD_{TH} within this range is linearly related to contrast (whether chromatic or luminance), a more traditional dimension for expressing sensitivity.

With the exception of the two conditions mentioned above (i.e., mask M3 and mixed sessions), the two authors served as observers for all the experiments. A few pilot sessions were also run with a naïve observer exclusively for stimulus configuration 6 (DCJ) in the C & O set. Vision was binocular with natural pupils.

3. PSYCHOPHYSICAL RESULTS

A. General Analysis

Figure 4 displays detection performances obtained with the large C & O set for both observers. Detection perfor-

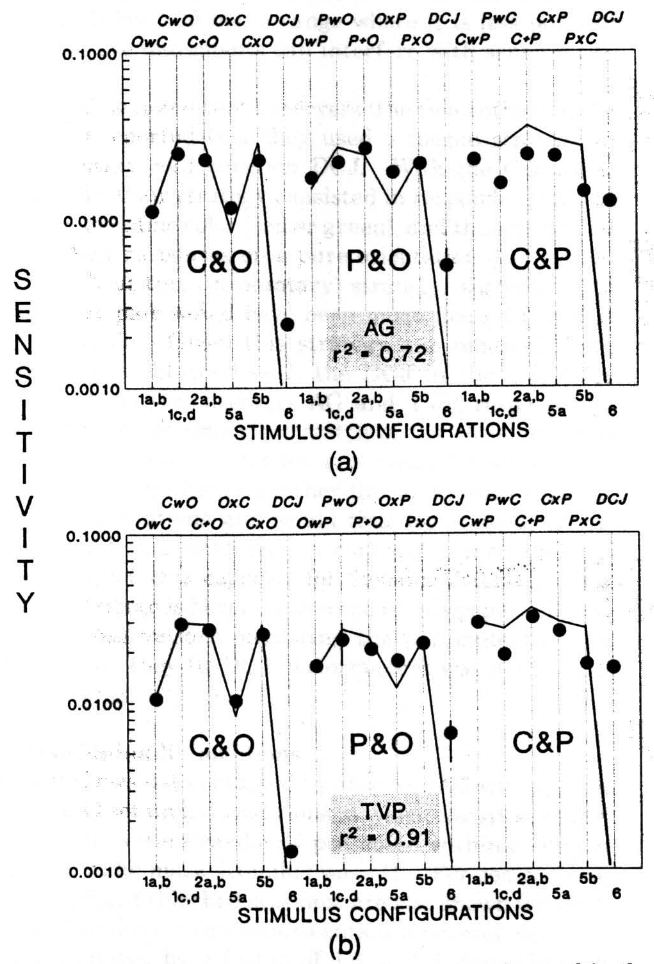

Fig. 5. Same as Fig. 4 but for the 18 texture pairs used in the limited C & O, P & O, and C & P sets.

mances for the limited C & O, P & O, and C & P sets are shown in Fig. 5. Psychophysical data (filled circles) should be distinguished from simulations (solid curves; discussed in Subsections 4.C and 4.D). Detection and identification performances (and slopes of the respective psychometric functions) were practically identical, so only the former are shown. The average values of β (pooled across all the experimental conditions) were 2.5 and 2.8 for observers AG and TVP, respectively. These average slopes correspond to average standard deviations of 31% and 27.5% of the mean, respectively. They are shown as vertical bars for two points in each plot of Figs. 4 and 5. As a general rule, AG and TVP performances are strongly correlated (Pearson correlations of $r^2 = 0.84$ for the complete C & O set of 11 conditions in Fig. 2 and of $r^2 = 0.94$ for the limited C & O, P & O, and C & P sets of 18 conditions in Fig. 3).

The analysis below is focused mainly on the data obtained with the limited C & O, P & O, and C & P sets (see Fig. 5). These data display the following general trends (note that the ordinate is logarithmic and that the vertical bars show ± 1 standard deviations and not ± 1 standard errors):

(1) The prior matching of performances for the C w O and P w O conditions did not produce a perfect match in the main experiments (compare sensitivities for these conditions for both observers in Fig. 5). This fact should explain a global but minor positive offset for all color-based (C & O set) discriminations relative to the polarity-based (P & O set) ones. The offset could be due to a mask-related effect, since the prior matching of the chromatic and luminance contrasts was obtained without masks (see Subsection 2.B).

(2) In the C & O and P & O sets discriminations based on color or polarity differences are always higher (for both observers) than those based on orientation, independent of whether the second attribute is uniform (w conditions) or varies randomly ($\times$ conditions) across the textures.

(3) Orientation-based discriminations are weaker (for both observers) under equiluminant (C & O set) conditions than under equichromatic (P & O set) conditions, which suggests a weak contribution of the CO units. However, performances with O w C and O $\times$ C are well beyond chance for both observers and support, together with our previous findings,[22] the existence of the CO mechanisms.

(4) In the C & P set color-based discriminations are systematically better than polarity-based ones. This difference is larger than that expected on the basis of a potential imperfect contrast-matching effect [see trend (1) above], and it could be accounted for, at least partly, by differences in the efficiency of mask M2 for stimulus sets P & O and C & P. However, the results of the control experiments described below (Subsection 3.C) reduce this possibility. Given our technique for assessing the equivalent luminance contrast of the chromatic stimuli (see Subsection 2.B), it is possible that this overall superiority of the color-based discriminations over the polarity-based discriminations in the C & P set reflects an imperfect pairwise matching of the activities in the oriented and nonoriented chromatic and luminance mechanisms.

(5) The covariance of two attributes (+ conditions) is expected (on grounds of probability summation) to improve discrimination performances relatively to conditions in which the textures in the texture pair differ in only one attribute (i.e., w conditions). With two exceptions (out of six; observer AG, P + O and C + P stimuli in the P & O and C & P sets) such improvement is not observed: performances with all the remaining + configurations are clearly not better than performances with the w configurations. While this counterintuitive result requires further testing, it can be predicted under the assumption that units that are simultaneously opponent in two dimensions (C & O, P & O, and C & P) do not exist or have insignificant weights (see Subsection 4.D). In fact, this assumption is required in the context of the model presented in Section 4 to account for the low performances obtained with all the DCJ stimuli.

(6) As one would expect, configurations DCJ yield by far the lowest segregation performances for both observers and for the three stimulus sets (see Figs. 4 and 5). SD thresholds for the DCJ of color and orientation were 280 and 445 ms with mask M1 and 433 and 773 ms with mask M2 for observers AG and TVP, respectively. For the mixed sessions the same configuration yielded a threshold of 670 ms (observer AG with mask M1; see Subsection 3.B). Despite fixation, eye movements might have been involved in all these durations. Data of this type have been previously taken as evidence for an independent processing of shape (orientation) and color.[28] The detection criteria with the DCJ of polarity and orientation and of color and polarity were reached by both observers for durations below 200 ms, a range where it is less but still likely that eye movements can interfere with sensitivity.

It should be noted that observers (the two authors and a naïve one) reported that they used a special strategy in discriminating configuration DCJ. With the C & O set, for example, their strategy consisted in responding only to textels of the same color (red or green), and thus they tried to base their responses on a pure orientation discrimination. Without this (involuntary) strategy, segregation of this texture pair would have been much more difficult if not impossible. Given this strategy, the relatively high performances obtained with the DCJ in the C & P set (81 and 64 ms for observers AG and TVP, respectively) may be due to the imperfect match of the chromatic and luminance contrasts. Indeed, any mismatch would help to focus one's attention on either the chromatic or the luminance modulations and would thus facilitate discrimination based on a difference in contrast in a single map. Accounting for this capacity for focusing attention on a specific attribute is beyond the scope of this paper. Based on these observations, adjusting the parameters of the model so that they fit DCJ performances was not considered a priority.

B. *Mixed-Stimuli Conditions*

Figure 6 shows data obtained by observer AG with the reduced C & O set under conditions in which the six stimulus configurations were randomly presented within a session (squares). The mask stimulus was M1. For comparison, data from Fig. 4 (blocked sessions) are also shown (circles). Mixing stimulus configurations entails an overall decrease of performances by a factor of 1.6 or 1.3, depending on whether or not configuration DCJ is taken into account. Mixing stimulus configurations does not change the rela-

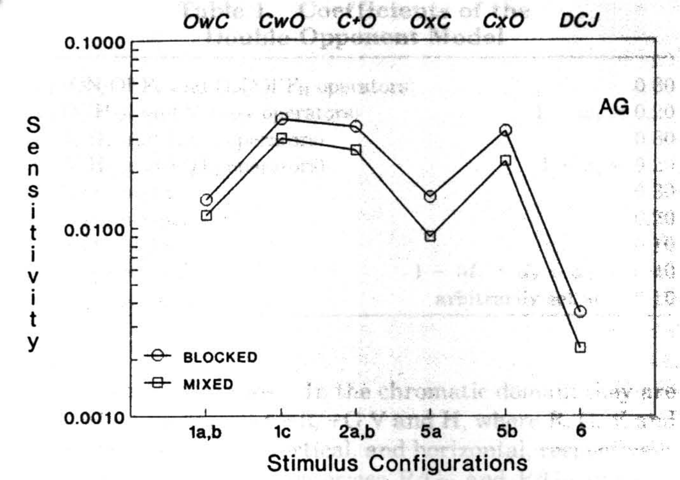

Fig. 6. Sensitivities (in inverse milliseconds) to the six texture pairs measured under both blocked (circles; redrawn from Fig. 4) and mixed (squares) conditions. The mask was of M1 type. The observer was AG.

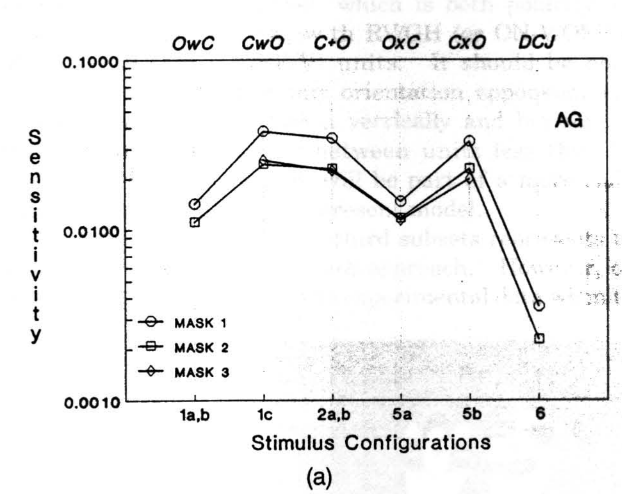

Fig. 7. Sensitivities (in inverse milliseconds) to six (or four for mask type M3) texture pairs with the mask type as a parameter. The observers were (a) AG and (b) TVP.

tive sensitivities to the six configurations, an observation that eliminates the possibility that the data collected in the blocked sessions are biased by nonsensory effects (i.e., the use of stimulus-specific discrimination strategies). As just noted above, this conclusion does not apply to configuration DCJ, for which such strategies have indeed been developed. For this texture pair the 81.6% discrimination criterion in the mixed sessions was reached for a stimulus duration of approximately 670 ms, a range where it is difficult to avoid eye movements. Sensitivity to this stimulus may thus be considered virtually zero and was considered such in the process of fitting our model to the data. As a consequence, the goodness of the fit was slightly worsened.

C. Different Masking Conditions

Figure 7 shows discrimination performances obtained with three types [observer AG, Fig. 7(a)] or two types [observer TVP, Fig. 7(b)] of mask for the restricted C & O set. Performances obtained with M1 masks are approximately 1.6 and 1.3 times higher (for observers AG and TVP, respectively) than those obtained with M2 and M3 masks; i.e., the latter two masks (observer AG only) yield practically identical performances. The main observation is that all the masks perserve the relative sensitivities for the selected stimulus configurations, discarding possible mask-related artifacts. This fact does not mean, of course, that the choice of a balanced mask for multiattribute stimuli is arbitrary. On the contrary, only a small set of masking configurations preserves the relative sensitivities, and their selection and use in our experiments was of primary concern. Our results demonstrate that, for the particular stimulation space used here, spatially distributed features built by means of a pairwise combination of the attributes that define the target texture (mask M1), of a local sum of these attributes (M3), or of a random spatial distribution of a larger set of attributes including those that define the target set (M2), provide fair (or balanced) masks. Fairness here refers to the property that the masks do not distort relative performances obtained with a large number of attribute combinations that define the set of target textures. This empirical observation might have theoretical implications relative to the nature of the attribute space under study and is of practical importance for future studies with multiattribute stimuli.

4. MODEL DESCRIPTION

The model that we describe in this section shares some basic features with previous models of texture discrimination[7-13] while adding new features related to color opponency, limited here to the red–green dimension, and to orientation opponency, limited here to vertical–horizontal interactions. Of course, one could relax these restrictions to incorporate the yellow–blue system as well as interactions between orientation-tuned channels that differ by one orientational bandwidth [as in Fig. 1(c)]. The limitation of our analysis is, however, justified by the limited attribute space used in our stimuli.

A. General Assumptions and Parameters

We postulate the existence of four distinct perceptual domains relevant to the types of texture used in the present experiments. These domains relate to CO, CnO, LO, and LnO populations of cells.[22,24]

We assume that each of the oriented domains consists of three distinct subsets (or maps). The first subset comprises the traditional oriented units (simple-cell-like), which are inherently polarity opponent. Such units may

Table 1. Coefficients of the Double-Opponent Model

w_1 (ON/OFF$_V$ and ON/OFF$_H$ operators)		0.80
w_2 (V/H$_{ON}$ and V/H$_{OFF}$ operators)	$1 - w_1 =$	0.20
z_1 (R/G$_V$ and R/G$_H$ operators)		0.80
z_2 (V/H$_R$ and V/H$_G$ operators)	$1 - z_1 =$	0.20
d_1 (LO weight)		0.30
d_2 (LnO weight)		0.20
d_3 (CO weight)		0.10
d_4 (CnO weight)	$1 - (d_1 + d_2 + d_3) =$	0.40
ϵ (Noise parameter)	arbitrarily set at	0.10

come in four varieties. In the chromatic domain they are +R/−G V and H, and −R/+G V and H, where R, G, V, and H denote red, green, vertical, and horizontal, respectively. In short, this subset comprises R/G$_V$ and R/G$_H$ units in the chromatic domain and ON/OFF$_V$ and ON/OFF$_H$ units in the luminance domain. The second subset comprises orientation-opponent units, i.e., V/H$_{R\,(\text{or ON})}$ and V/H$_{G\,(\text{or OFF})}$ (also in four varieties). For completeness, we assume the existence of a third subset, which is both polarity and orientation opponent, i.e., with RV/GH (or ON-V/OFF-H) and RH/GV (ON-H/OFF-V) units. It should be noted that, for simplicity, the only orientation opponency considered here is that between vertically and horizontally tuned units. Opponency between units less than 90° apart [see Figs. 1(c) and 8] will be part of a more elaborated, analog version of the present model.

The use of the second and third subsets represents the main innovation of the present approach. However, our model provided best fits of the experimental data when the contribution of the third subset was set virtually to zero, which implies that units that are simultaneously polarity (or color) and orientation opponent might not exist. So, having started with three subsets, we ended with only two subsets (or maps) per domain. This particular point is discussed in more detail in Subsection 4.D.

Within each subset of the LO and CO domains it is assumed that all the units have equal weights. Under the assumption that the third subset does not exist, the model requires the adjustment of eight coefficients, of which four represent the relative weights of the two subsets within each oriented domain and four represent the relative weights of the four (LO, LnO, CO, and CnO) domains. In fact, we can see that this number reduces to 5. Since the subset weights are relative, they should sum to unity within each domain, which leaves only one subset free parameter per domain, i.e., two subset coefficients (w and z). Identically, the domain weights should also sum to unity, which leaves only three domain free parameters (d). Thus there are five coefficients altogether (see Table 1). A sixth parameter, related to the noise in the system, may or may not be necessary, depending on the specific computation that determines the texture gradient (see Subsection 4.A). The number of free parameters is reasonably low, given that we required that the model fit 23 experimental conditions.

B. Flow Chart

A simplified schematic of the model is shown in Fig. 8.

First Stage. Linear convolution with oriented and nonoriented ON and OFF units is performed in both the luminance and the chromatic domains.

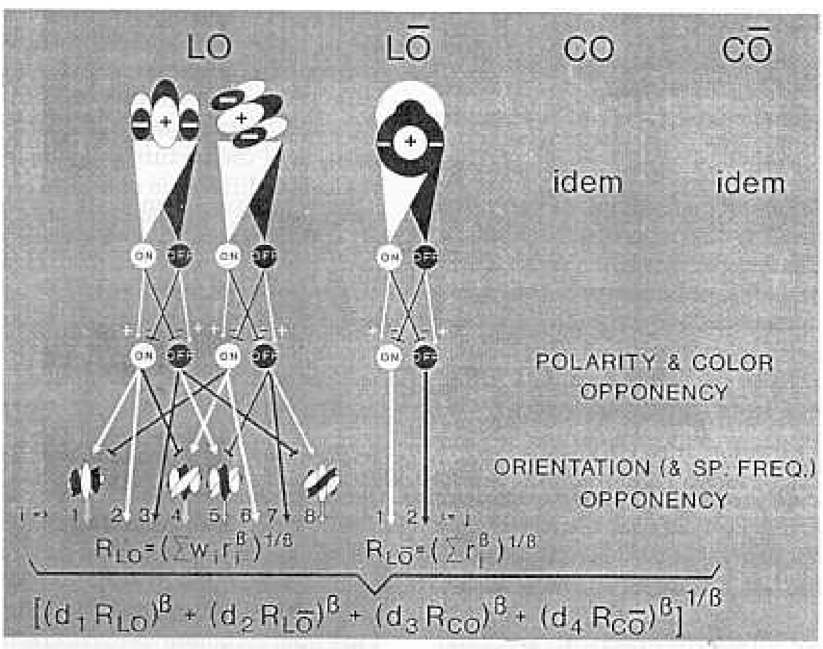

Fig. 8. Flow chart of the double-opponency model shown only for the LO and LnO (≡L$\bar{O}$) domains. Identical schemes apply to the CO and CnO (≡C$\bar{O}$) domains. It is understood that the first-order receptive fields shown at the top for each domain occupy the same retinal location. Thus, up to the third processing stage (see below), this diagram illustrates only local operations. Within each domain linear ON- and OFF-center units (first processing stage) inhibit each other (differencing operation) to produce half-wave rectified units at a second processing stage. These units may have direct output (see the arrows numbered 2 and 3 and 6 and 7 for the LO domain and 1 and 2 for the LnO domain) or interact at the third processing stage, where inhibition (or differencing) occurs between units of the same polarity but of different orientation (see the arrows numbered 1, 4, 5 and 8 in the LO domain) and between units that differ in both orientation and polarity (not shown). A texture-gradient response r is computed at a fourth stage from the final outputs of each operator across the space (in both oriented and nonoriented domains), and the responses r_i and r_j are summed probabilistically within each domain (β summation; fifth stage). Finally, weighted texture-gradient responses R of each domain are also summed probabilistically (sixth stage; in principle, orientation opponency could be generalized to spatial frequency or other second-order dimensions).

Second Stage. At each spatial location the outputs of ON (or red) and OFF (or green) nonoriented and oriented units are differenced so that we obtain ON and OFF half-wave rectified units. Half-wave rectification is typical of simple V1 cells whose behavior is supposedly mimicked by this processing stage.[10,36] At this point both the oriented and the nonoriented units are already polarity opponent, and their outputs are conveyed without further transformation to the next stage [see the long arrows numbered 2 and 3 and 6 and 7 for LO and 1 and 2 for LnO (labeled LO) in Fig. 8]. Of course, half-wave rectification could have been implemented from the beginning considering that lateral geniculate cells have a rather low resting discharge.

Third Stage. Half-wave rectified oriented filters that differ in either orientation or both orientation and polarity interact through the same differencing operation as that in the second stage and produce at each spatial position (in both the LO and CO domains) eight additional opponent filters, four of which are the complements of the others. For simplicity, Fig. 8 displays only the orientation-opponent receptive fields numbered 1, 4, 5, and 8 (LO domain). Also for simplicity, Fig. 8 displays only the center of the second-order receptive fields. The surround, which displays opposite-sign response profiles, was exemplified in Fig. 1(c). While the receptive fields of the third-stage operators could not be represented graphically in Fig. 8 as the linear sum of the Gabor-like, first-order receptive fields, it should be noted that they are reminiscent of the classical complex-cell receptive field [see Fig. 1(c) for the correct representation].

Fourth Stage. A texture gradient, or edge, is computed for each operator by the use, as a rule of thumb, of both the difference between the output across the edge and the smallest of the average signals within each texture of the texture pair, or the ratio between this difference and the smallest average signal (i.e., normalization; see Subsection 4.C). Since this smallest average signal may be null, the ratio computation requires an additional noise parameter (ϵ). The ratio computation implies a Weber-like behavior that could account for some of the texture discrimination asymmetries mentioned in the literature.[25] Extracting the texture edge independently in complementary operators (e.g., ON and OFF units) ensures that spatial phase information is preserved.

Fifth Stage. Texture-gradient signals are weighted and summed probabilistically (β summation)[34] within each domain. The weights (w_i for LO domains and z_i for CO domains) determine the relative contributions of the different operator subsets in each domain and are parameters of the model. The probability summation accounts for the degree of independence of the operators and/or for an intrinsic nonlinearity of the operators themselves.[37] The β parameter was estimated experimentally for each observer.

Sixth (and Last) Stage. Texture gradients are also probabilistically summed across domains, where each domain's sum is given a specific weight d_i.

C. Computational Implementation

We estimated the performance of the model by using a statistical approach. Rather than actually convolving the image with spatially extended filters, as suggested in Fig. 3, we estimated the output of such filters assuming that their spatial extent was precisely matched to the intertexel distance. To be specific, let us consider a red–green double-opponent operator, which has an excitatory response to a red light and an inhibitory response to a green light at its center x, with the opposite response signs at $x + \Delta x$. We obtained the response of this operator by sampling only at the two points x and $x + \Delta x$, where the two textels are assumed to be located, and this response will yield a rough approximation to the expected response of an analog filter. The output at x is arbitrarily set to a maximum of $+1$ for a red textel and -1 for a green textel, with a linear variation between, i.e., a zero response for yellow; of course, the zero response may be offset by the spontaneous firing rate, which changes the response range to 0–2. We chose to consider each operator as a half-wave rectifier with positive responses in the range 0–1. The response of other double-opponent operators is computed analogously.

For simplicity, let us assume that the texture pair consists of two textured regions, T_l on the left-hand side and T_r on the right-hand side, separated by a vertical edge G. The expected values of the operators' responses, based on the types and the relative probability densities of the textels that form the texture pair, are found as follows:

(1) Find the expected value E for the output H_q of each operator q across all possible textel pairs within T_l (and T_r). As an example, for the left-hand texture we obtain

$$E_l = \text{Average}[(H_q)_l] = \sum_{i\in T_l}\sum_{k\in T_l} n_i n_k H_q(i,k),$$

where n_i and n_k are the probabilities of the two textels and $H_q(i,k)$ is the output of the operator when it spans textels i and k. This procedure is repeated for the expected output E_r inside the right-hand region and for E_G across the texture edge. Values for E_l, E_r, and E_G are computed individually for each operator in all the domains.

(2) The magnitude of the texture gradient, M_G, i.e., the strength of the texture edge for each operator, is obtained by either a difference or a ratio estimator. For the difference measure, M_G is simply set to $E_G - E_{\min}$, where $E_{\min}$ is the minimum between E_l and E_r; for the ratio measure, M_G is set to $(E_G - E_{\min})/E_{\min}$.

(3) Combine the edge strengths of all individual operators within a domain through a β summation:

$$\text{Domain}(M_G) = \left[\sum_{q\in\text{domain}} d_G(M_{G,q})^{\beta}\right]^{1/\beta},$$

where $M_{G,q}$ is the signal strength of the qth operator within the domain under consideration and d_G is its weight.

(4) Finally, the overall signal strength is obtained by a β summation across all the domains.

The model in its present form is discrete and statistical. This approach may be criticized on different grounds, but our claim is that it is predictive of the crude behavior of a more elaborated, multiscale analog model (see, for example, Refs. 9 and 13 for a similar approach), which we are pursuing.

D. Predictions of the Model

As we discussed in Subsection 4.B, the free parameters of the model refer to the relative weights of the opponent op-

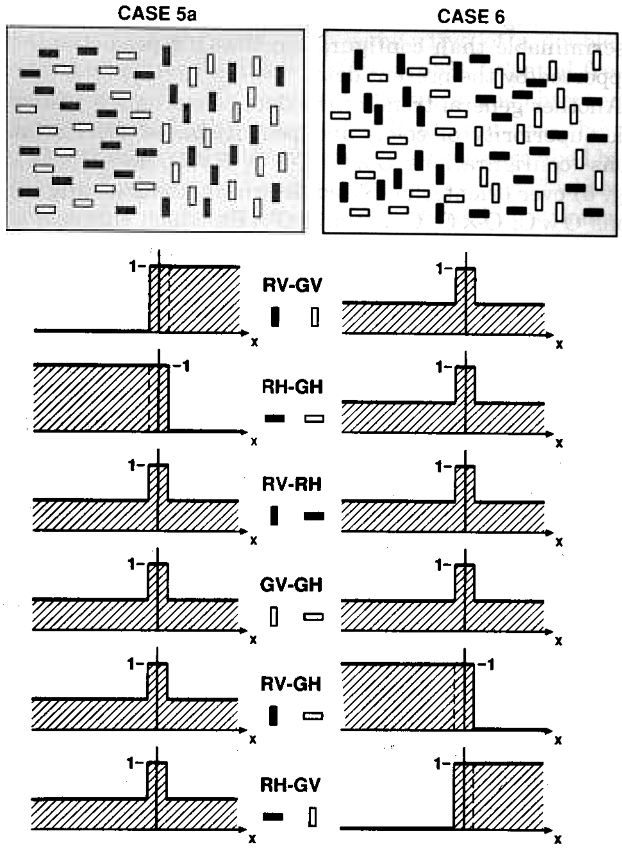

Fig. 9. Oriented units that differ at the same time in their orientation and color (or polarity) probably do not interact. The average outputs of the eight possible differencing operations (denoted in the middle of the figure) between units specified by their preferred color [red (R) or green (G)] and orientation [horizontal (H) or vertical (V)] are shown for texture pairs 5a (O × C) and 6 (DCJ). Texture gradients summed across the eight operators produce equally strong signals for both texture pairs. The only way of accounting for the obvious discriminability difference between these texture pairs is to assume low or null weights for operators RV/GH and RH/GV. See the text for details.

erators within the LO and CO domains (w_i and z_i, respectively), to the relative weights d_i of the four considered domains (LO, LnO, CO, and CnO), and to the noise-related parameter ϵ. The last-named was arbitrarily set at 0.1 (i.e., 10% of the maximum output of any operator), and it is not considered in the following discussion.

Figure 9 illustrates our claim that oriented operators that are simultaneously opponent in color (or polarity) and orientation (i.e., RV/GH and RH/GV units and their ON and OFF counterparts) should not be considered in the framework of the present model. Figure 9 displays the outputs of the six possible combinations of red/green and vertical/horizontal units that yield double opponency in response to configurations O × C and DCJ. As one can note by mere inspection (and as confirmed by the data in Figs. 4 and 5), it is significantly more difficult to discriminate texture pair DCJ than texture pair O × C. This is the case whether the textures are shown with different colors or with different polarities (as illustrated). However, the simple summation (whether linear or not) of the signals at the texture edges computed from the six outputs will yield identical responses for the two texture pairs. Within the context of the model, the only way that one can account for the actual percept is to decrease the weights to the RV/GH and RH/GV operators. If performances with configuration DCJ are close to those that arise from chance (as we suspect they are, at least for the C & O set), these weights should be set to zero. With zero weights, discrimination of configuration O × C will be clearly favored over that of configuration DCJ. Setting RV/GH and RH/GV weights to zero would also account for the unexpected lower performances with configuration C + O relative to configuration C w O (see Figs. 4–7). Indeed, the model predicts higher performances for the former, given the stronger activation of RV/GH and RH/GV units. If these units do not exist, or if their weight is relatively small, the correct, albeit counterintuitive, predictions are obtained.

Finally, it should be noted that not all DCJ stimuli are necessarily undiscriminable by human observers.[30,31,38] Thus operators that are opponent in more than one dimension (e.g., disparity and direction) may actually exist, and the present model should account for performances with such DCJ stimuli by simply assigning nonzero weights to the relevant operators. By comparison, a standard energy computation approach[9,11] is bound to predict zero discrimination for any DCJ configuration. Indeed, ignoring the sign of the textels of the DCJ configuration in Fig. 9 will produce a spatially unmodulated activity in both the vertical and horizontal maps and will thus lead to zero discrimination.

The five free parameters of the model were estimated by successive (but not exhaustive) iterations. Remarkably, the best fit to the data of both observers was obtained with the same set of coefficients (to the first decimal; see Table 1).

Difference and ratio predictions of the model are virtually identical, with one exception for condition DCJ, for which the former systematically overestimates measured performances and the latter underestimates them. For reasons given in Subsection 4.B we preferred the second alternative and therefore show only the ratio predictions (solid curves in Figs. 4 and 5). The correlations between the ratio simulations and the psychophysical data obtained with the complete C & O set (11 stimulus configurations) are 0.91 and 0.79 for observers AG and TVP, respectively. The correlations between simulations and the psychophysical data obtained with the limited C & O, P & O, and C & P sets (18 configurations) are 0.72 and 0.91 for observers AG and TVP, respectively. The average correlation (across observers and stimulus sets) of 83.25 compares favorably with those found by Rubenstein and Sagi[11] (0.80; p. 1638) and by Malik and Perona[10] (81.5; computed from their Table 3). It should be noted that these correlations would have been improved had we adjusted the parameters of the model to obtain better fits for the DCJ conditions. As we mentioned in Subsection 4.B, the ratio (as opposed to the difference) variant is *a priori* more reasonable, since it produces a Weber-like behavior in texture discrimination, which, in turn, might account for some asymmetrical pop-out effects[25] recently discussed from a theoretical point of view by Rubenstein and Sagi.[11]

Based on the large number of iterations performed with different parameter sets, it appears that globally good fits of the data always require that the weight of the CO domain be significantly lower than the remaining three weights and that the CnO weight be stronger than the LnO weight. The first finding is consistent with the neurophysiological literature,[29,39] while the validity of the second finding requires additional neurophysiological evidence. It is important to note that, if the contribution of the CO domain is arbitrarily set to zero, the model predicts null sensitivities for configurations O w C and O × C (see Figs. 4–6). The experimental data show relatively high sensitivities for these stimuli and confirm, together with previous studies,[22,40] the existence of CO mechanisms. A good fit of the data also requires that the weights of the orientation-opponent interactions in both the chromatic- and luminance-oriented domains (i.e., parameters w_2 and z_2) be weaker than the weights of the polarity interactions within the same domains (i.e., parameters w_1 and z_1). The interpretation of this observation is that vertical–horizontal interactions are substantially weaker than interactions between units of the same orientation but of opposite polarity (or color). This behavior can be understood if one assumes that, as suggested by recent electrophysiological data,[19] the strongest orientational interactions occur between orientation-tuned channels that differ by less than 90° (i.e., by one orientational bandwidth).

Whether the fitted parameters can be regarded as valid estimators of the relative proportions of the underlying cell populations remains a question that will be answered by the behavior of a more comprehensive, analog version of the present model tested against additional electrophysiological data.

5. DISCUSSION

Some of the stimulus configurations used in the present study may be regarded as generalizations of more traditional stimuli used in visual-attention, "odd man out" experiments (SCJ and DCJ, represented in Fig. 2 by configurations 4a and 4b and by configuration 6, respectively). As such, they contribute to our understanding both of multiattribute interactions in spatial vision and of the underlying mechanisms. Taken at face value, the present results lead to the following conclusions.

The data clearly support the existence of chromatic-oriented mechanisms. Units of this type are absolutely necessary in accounting for the discrimination of texture pairs such as O w C and O × C. Indeed, these equiluminant texture pairs differ only in their orientation, and their discrimination requires units that are both orientation and chromatic specific. One may argue that chromatic broadband units would do equally well. Independent of their unlikely existence,[6,41] we found at least two reasons to discard them. The first relates to the so-called veto effect that we reported earlier in both motion and texture studies.[22,24,42] The term veto refers to the fact that, under equiluminant conditions, orientation matching cannot carry motion or yield spatial grouping if color is mismatched. Chromatic broadband oriented units should, however, ignore color mismatch and yield both motion perception and perceptual grouping under such conditions. A second argument against implementation of broadband oriented units in the model was based on the present data. These units cannot discriminate configuration C w O, whereas they respond strongly to configuration C + O. If broadband chromatic units were to replace the CO units, configuration C + O should be significantly more discriminable than configuration C w O, a prediction not supported by the present data.

Another general trend of the data concerns the systematic superiority of color- and polarity-based discriminations (configurations C w O, C × O, P w O, and P × O in Fig. 5) over orientation-based discriminations (configurations O w C, O × C, O w P, and O × P), which suggests an overall smaller contribution of the oriented mechanisms.[43] Sensitivities measured with the C & P stimulus set indicate that, when color and polarity are combined, the contribution to texture discrimination of the former (and, presumably, of the underlying mechanisms) is always stronger than the contribution of the latter, despite the fact that their respective contrasts have been matched for equal performances. Our model accounts for this fact by assigning stronger weights to the CnO domain than to the LnO domain. While some neurophysiological studies appear to support (at least qualitatively) this possibility,[29,44–46] other accounts definitely reject it[6,41] (see below).

The two control experiments (Figs. 6 and 7) present some methodological interest. The first one (Fig. 6) revealed that observers develop stimulus-related strategies only for the DCJ configuration, in that they may attend to a given color (or polarity) and base their responses on an orientation (or color) difference. This observation bears on the characteristics of visual attention and deserves further investigation. The second control experiment (Fig. 7) showed that, for the present set of multiattribute target stimuli, there is a set of balanced mask stimuli that yield equivalent relative masking effects. This observation may be interpreted in relation to the topology of the multidimensional sensory space within which these attributes are located, but the limited set of experimental conditions studied here does not permit elaboration on this particular topic. The multiple mask experiments provide, nonetheless, a basis for the choice of masks in further studies.

The model that we have developed leans heavily on the concept of generalized double opponency. While the traditional understanding of double-opponent units (which requires that opposite-sign responses be processed independently) may render this concept inappropriate for the characterization of the classical (lateral geniculate and V1) ON–OFF achromatic units, it is clear that such units may be regarded as spatial contrast measuring devices in the luminance domain. On the other hand, the existence of classical double-opponent units that perform the equivalent task in the chromatic domain has been a matter of recent debate.[6,41] The significant characteristic of the double-opponent unit is its spatial opponent behavior. Whether or not the response of the double-opponent unit undergoes some nonlinear transformations (such as half-wave rectification), the unit's capacity for computing spatial contrast will not be impaired. The nonlinear behavior of cortical units may be one reason why, using different stimulation techniques, different authors[6,29,41,44–46] arrived at opposite conclusions about the existence of prototypical chromatic double-opponent cells. At any rate, the extensive analysis of the chromatic properties of cortical neurons provided by Lennie *et al.*[6] clearly supports the existence of simple cells that prefer chromatic to achromatic modulations and are "more sensitive to some chromatic grating [between 2 and 4 cycles/deg;

see Fig. 16 of Ref. 6] than to chromatic modulation of a spatially uniform field" (i.e., supportive of a double-opponent receptive field; see Ref. 6, p. 663). Spatial frequency selectivity with chromatic gratings was observed by Lennie *et al.*[6] with complex cells as well (see their Fig. 17). Finally, receptive fields of the type described by Hubel and Livingstone[47] and by Ts'o and Gilbert,[48] whose surround only suppresses the activity elicited by stimulation of their chromatically opponent center, may well be looked on as half-wave rectified, double opponent.

Ingling and Martinez-Uriegas[49] provided a theoretical analysis that demonstrated why an ideal type I cell should be regarded as a general-purpose double-opponent device. Along this line of reasoning we assumed that double opponency could be extended to second-order features such as orientation, spatial frequency, and even motion. This idea is not new (see Ref. 50 for a review) and has recently received strong psychophysical support.[16–18,26,27] However, it may be more difficult to characterize second-order opponencies than first-order ones. In the orientation domain, for example, recent data[17,18,21,51–53] suggest that same-orientation, nonoverlapping stimuli may facilitate each other if they are collinear and inhibit each other if they are parallel. Only the second type of interaction has been considered in the present model. Testing and modeling these anisotropic interactions remain matters of further investigation.

ACKNOWLEDGMENTS

We thank Bela Julesz for his kind and insightful support and Ilona Kovacs, Larry Maloney, Sophia Würger, Ken Knoblauch, Dov Sagi, and Barton Rubenstein for their helpful comments while this study was in progress. Akos Feher's enthusiasm and computer skills were invaluable in the construction of our stimuli. This research was supported by grants BNS-9109384 (National Science Foundation), N00014-92-J-1312 (U.S. Office of Naval Research), and (for A. Gorea) 91-074 (Direction des Recherches, Etudes et Techniques—Ministère de la Défense). Preliminary reports of this study were given at three conferences.[54]

REFERENCES AND NOTES

1. E. Hering, *Outlines of a Theory of the Light Sense*, L. M. Hurvich and D. Jameson, translators (Harvard U. Press, Cambridge, Mass., 1964), pp. 49–50 and 176–181.
2. N. W. Daw, "Goldfish retina: organization for simultaneous color contrast," Science **158**, 942–944 (1967).
3. D. H. Hubel and T. N. Wiesel, "Receptive fields and functional architecture of monkey striate cortex," J. Physiol. (London) **195**, 215–243 (1968).
4. D. Jameson, "Opponent-colours theory in the light of psychophysical findings," in *Central and Peripheral Mechanisms of Colour Vision*, D. Ottosin and S. Zeki, eds. (Macmillan, London, 1985), pp. 83–102.
5. G. Sperling, "Three stages and two systems of visual processing," Spatial Vis. **4**, 183–207 (1989).
6. P. Lennie, J. Krauskopf, and G. Sclar, "Chromatic mechanisms in striate cortex of macaque," J. Neurosci. **10**, 649–669 (1990).
7. J. R. Bergen and E. H. Adelson, "Early vision and texture discrimination," Nature (London) **333**, 363–364 (1988).
8. H. Voorhees and T. Poggio, "Computing texture boundaries from images," Nature (London) **333**, 364–367 (1988).
9. I. Fogel and D. Sagi, "Gabor filters as texture discriminators," Biol. Cybern. **61**, 103–113 (1989).
10. J. Malik and P. Perona, "Preattentive texture discrimination with early vision mechanisms," J. Opt. Soc. Am. A **7**, 923–932 (1990).
11. B. S. Rubenstein and D. Sagi, "Spatial variability as a limiting factor in texture-discrimination tasks: implications for performance asymmetries," J. Opt. Soc. Am. A **7**, 1632–1643 (1990).
12. M. S. Landy and J. R. Bergen, "Texture segregation and orientation gradient," Vision Res. **31**, 679–691 (1991).
13. N. Graham, J. Beck, and A. Sutter, "Nonlinear processes in spatial-frequency channel models of perceived texture segregation: effects of sign and amount of contrast," Vision Res. **32**, 719–743 (1992).
14. The inhibitory interactions postulated by Landy and Bergen[12] between units tuned to different orientations lack spatial opponency.
15. D. Sagi and S. Hochstein, "Lateral inhibition between spatially adjacent spatial-frequency channels?" Percept. Psychophys. **37**, 315–322 (1983).
16. C. Chubb, G. Sperling, and J. A. Solomon, "Texture interactions determine perceived contrast," Proc. Natl. Acad. Sci. USA **86**, 9631–9635 (1989).
17. M. W. Cannon and S. C. Fullenkamp, "Spatial interactions in apparent contrast: inhibitory effects among grating patterns of different spatial frequencies, spatial positions and orientations," Vision Res. **31**, 1985–1998 (1991).
18. U. Polat and D. Sagi, "Lateral interactions between spatial channels: suppression and facilitation revealed by lateral masking," Invest. Ophthalmol. Vis. Sci. Suppl. **33**, 1345 (1992).
19. A. B. Bonds, "Role of inhibition in the specification of orientation selectivity of cells in the cat striate cortex," Vis. Neurosci. **2**, 41–55 (1989).
20. L. A. Bauman and A. B. Bonds, "Inhibitory refinement of spatial frequency bandpass of single cells in the cat striate cortex," in *Seeing Contour and Colour*, J. J. Kulikowski, C. M. Dickinson, and I. J. Murray, eds. (Pergamon, Oxford, 1989), pp. 81–84.
21. D. C. Van Essen, E. A. DeYoe, J. F. Olavarria, J. J. Knierim, and B. Julesz, "Neural responses to static and moving texture patterns in visual cortex of the macaque monkey," in *Structure and Function of the Visual Cortex*, D. M. K. Lam and C. Gilbert, eds. (Portfolio, The Woodlands, Tex., 1989), pp. 137–154.
22. A. Gorea and T. V. Papathomas, "Texture segregation by chromatic and achromatic visual pathways: an analogy with motion processing," J. Opt. Soc. Am. A **8**, 386–393 (1991).
23. W. McIlhagga, T. Hine, G. R. Cole, and A. W. Snyder, "Texture segregation with luminance and chromatic contrast," Vision Res. **30**, 489–495 (1990).
24. A. Gorea and T. V. Papathomas, "Motion processing by chromatic and achromatic visual pathways," J. Opt. Soc. Am. A **6**, 590–602 (1989).
25. D. Williams and B. Julesz, "Filters versus textons in human and machine texture discrimination," in *Neural Networks for Perception*, Vol. I of Human and Machine Perception, H. Wechsler, ed. (Academic, Boston, Mass., 1991), pp. 145–147.
26. A. B. Watson, "Motion pooling areas estimated from motion-contrast sensitivity functions," Invest. Ophthalmol. Vis. Sci. Suppl. **33**, 974 (1992).
27. I. Murakami and S. Shimojo, "Directionally selective mechanisms modulated by surrounding motion are underlying motion capture, induced motion and motion aftereffect," Invest. Ophthalmol. Vis. Sci. Suppl. **33**, 1137 (1992).
28. A. Treisman and G. Gelade, "A feature-integration theory of attention," Cognit. Psychol. **12**, 97–136 (1980).
29. M. S. Livingstone and D. H. Hubel, "Anatomy and physiology of a color system in the primate visual cortex," J. Neurosci. **4**, 309–354 (1984).
30. A. Treisman and S. Sato, "Conjunction search revisited," J. Exp. Psychol. Human Percept. Psychophys. **16**, 459–478 (1990).
31. J. M. Wolfe, K. R. Cave, and F. L. Franzel, "Guided search: an alternative to the feature integration model of visual search," J. Exper. Psychol. Human Percept. Perform. **15**, 419–433 (1989).
32. E. Switkes, A. Bradley, and K. K. De Valois, "Contrast de-

pendence and mechanisms of masking interactions among chromatic and luminance gratings," J. Opt. Soc. Am. A **5**, 1149–1162 (1988).
33. C. Agonie and A. Gorea, "Equivalent luminance contrast of red–green drifting stimuli: dependency on luminance-color interactions and on the psychophysical task," J. Opt. Soc. Am. A **10**, 1341–1352 (1993).
34. A. B. Watson, "Probability summation over time," Vision Res. **19**, 515–522 (1979).
35. A. Gorea and C. W. Tyler, "New look at Bloch's law for contrast," J. Opt. Soc. Am. A **3**, 52–60 (1986).
36. D. J. Heeger, "Computational model of cat striate physiology," in *Computational Models of Visual Perception*, M. S. Landy and J. A. Movshon, eds. (MIT Press, Cambridge, Mass., 1991), pp. 119–133.
37. H. R. Wilson, "A transducer function for threshold and suprathreshold human vision," Biol. Cybern. **38**, 171–178 (1980).
38. K. Nakayama and G. H. Silverman, "Serial and parallel processing of visual feature conjunctions," Nature (London) **320**, 264–265 (1986).
39. L. G. Thorell, R. L. De Valois, and D. G. Albrecht, "Spatial mapping of monkey V1 cells with pure color and luminance stimuli," Vision Res. **24**, 751–769 (1984).
40. P. Cavanagh, M. Arguin, and A. Treisman, "Effect of surface medium on visual search for orientation and size features," J. Exper. Psychol. Human Percept. Perform. **16**, 479–491 (1990).
41. P. Lennie and M. D'Zmura, "Mechanisms of color vision," CRC Crit. Rev. Neurobiol. **3**, 333–400 (1988).
42. A. Gorea and T. V. Papathomas, "The concept of 'veto'-attributes in motion perception," Invest. Ophthalmol. Vis. Sci. Suppl. **29**, 265 (1988).
43. While we did match chromatic and luminance contrasts (see Subsection 2.B), we do not have a metric to compare them with the 90° orientation contrast. We do know that the latter is at its maximum value. It may then be stated safely that, at least at the spatial scale at which the textels were visible, units that permit orientation-based discriminations provide weaker output than units that permit color- and polarity-based discriminations.
44. C. R. Michael, "Color vision mechanisms in monkey striate cortex: dual-opponent cells with concentric receptive fields," J. Neurophysiol. **41**, 572–588 (1978).
45. C. R. Michael, "Color vision mechanisms in monkey striate cortex: simple cells with dual opponent-color receptive fields," J. Neurophysiol. **41**, 1233–1249 (1978).
46. C. R. Michael, "Color-sensitive complex cells in monkey striate cortex," J. Neurophysiol. **41**, 1250–1266 (1978).
47. M. S. Livingstone and D. H. Hubel, "Segregation of form, color and stereopsis in primate area 18," Science **240**, 740–749 (1988).
48. D. Y. Ts'o and C. D Gilbert, "The organization of chromatic and spatial interactions in the primate striate cortex," J. Neurosci. **8**, 1712–1727 (1988).
49. C. R. Ingling, Jr., and E. Martinez-Uriegas, "The spatiotemporal properties of the r-g X-channel," Vision Res. **25**, 33–38 (1985).
50. J. Allman, F. Miezin, and E. McGuinness, "Stimulus specific responses from beyond the classical receptive field: neurophysiological mechanisms for local–global comparisons in visual neurons," Annu. Rev. Neurosci. **8**, 407–430 (1985).
51. D. J. Field, A. Hayes, and R. F. Hess, "The glue in fractal edges: an example of feature integration by the human visual system," Invest. Ophthalmol. Vis. Sci. Suppl. **33**, 1347 (1992).
52. H. C. Nothdurft, "Sensitivity for structure gradient in texture discrimination tasks," Vision Res. **25**, 1957–1968 (1985).
53. H. C. Nothdurft, "Texture segmentation and pop-out from orientation contrast," Vision Res. **31**, 1073–1078 (1991).
54. 13th European Conference on Visual Perception, Vilnius, Lithuania, August 26–30, 1991; Contrasts in Vision, Cambridge, UK, September 4–6, 1991; Annual Meeting of the Optical Society of America, San Jose, Calif., November 3–8, 1991.